DALTON
FULL PAPER

Hydrothermal synthesis and characterisation of alkaline-earth metal salts of benzene-1,3,5-tricarboxylic acid

M. John Plater,* Alexander J. Roberts, Jim Marr, Eric E. Lachowski and R. Alan Howie

Department of Chemistry, University of Aberdeen, Meston Walk, Old Aberdeen, UK AB24 3UE

The reaction of M^{II} acetate (M = Sr or Ba) with benzene-1,3,5-tricarboxylic acid (H_3btc) yielded crystals of formulae $[M(Hbtc)(H_2O)_2]\cdot 0.5H_2O$. These compounds are isostructural as shown by X-ray single-crystal analysis and by X-ray powder diffraction patterns. The structures consist of alternating layers of parallel Hbtc anions and cations stacked along the *c* axis. The metal ions are co-ordinated by two bidentate carboxylate groups, three monodentate carboxylate groups and two water molecules giving an overall co-ordination number of nine. Heating liberates 2.5 water molecules per formulae unit to give M(Hbtc) which can reversibly bind water reforming $[M(Hbtc)(H_2O)_2]\cdot 0.5H_2O$.

Metal-ion directed assembly of organic molecular building blocks known as 'tectons' is giving access to new open-framework solid-state materials with fascinating technological potential and scientific interest.[1] The synthesis of one-, two- and three-dimensional co-ordination polymers which are structurally analogous to important minerals such as quartz, clays and zeolites[2] requires rigid tectons which possess divergent functional groups. In open-framework co-ordination polymers metal ions form ionic bridges or co-ordinative bonds which link the rigid tectons together. Some organic building blocks or 'tectons' used to date and the corresponding metal-ion salts include pyrazine with $AgPF_6$[3a] or $Co(NCS)_2$,[3b] bipyridyl with $M(NO_3)_2$ (M = Co, Ni or Zn)[4] $Co(NCS)_2$,[3b] $Cu(NO_3)_2$,[5a] CuCl,[5b] $[Zn(H_2O)_6][SiF_6]$,[6] or $Cd(NO_3)_2$,[7] pyrimidine with $[Cu(CH_3CN)_4][BF_4]$,[2a] 2,4,6-tri(4-pyridyl)-1,3,5-triazine with $Zn(NO_3)_2$ and NEt_4CN,[8] 1,4-bis(4-pyridyl)butadiyne with $Cd(CN)_2$,[9] 1,3,5-tricyanobenzene or 1,3,5-tri(4-ethynylbenzonitrile)benzene with $AgCF_3SO_3$,[1e] benzene-1,3,5-tricarboxylic acid (H_3btc) with $Co(O_2CMe)_2$,[10] $Zn(O_2CMe)_2$, $Ni(O_2CMe)_2$ or $Ca(O_2CMe)_2$,[11] squaric acid (3,4-dihydroxycyclobut-3-ene-1,2-dione) with $CoCl_2$,[12a] $Ba(NO_3)_2$ and $Sr(NO_3)_2$,[12b] croconic acid with $MnCl_2$,[12c] 2,5-dihydroxy-*p*-benzoquinones with $Ba(NO_3)_2$, $Cd(NO_3)_2$ and $Mn(NO_3)_2$,[12d] pyridine-2,3-dicarboxylic acid with $ZnCl_2$ or $MnCl_2$[13a] and pyridine-3,5-dicarboxylic acid with $Co(O_2CMe)_2$.[13b] Some materials have shown promising applications such as ion exchange,[5a] selective guest absorption[14] and heterogeneous catalysis.[7] An organic zeolite with large pores, without an interpenetrating lattice, was recently prepared by crystallisation of H_3btc with cobalt nitrate and pyridine.[14] The organic pyridine templates were subsequently removed from the lattice by heating. The 'activated' zeolite was able reversibly to absorb aromatic compounds. This methodology resembles that used for aluminosilicate zeolites which are frequently formed with an organic template which can be subsequently removed from the lattice.[2b] In contrast, although many organic clathrates are known, which are stabilised by hydrogen bonding and van der Waals forces, if the 'template' or guest molecules can be removed by heating the supramolecular hydrogen-bonded network is not strong enough to sustain the void volume that is left.[15] Polar tectons such as H_3btc[16] or atamentane tetracarboxylic acid (H_4atc)[17] also crystallise with hexagonal and diamondoid interpenetrating lattices respectively which minimise the void volume in the lattice. If H_3btc crystallised forming the so-called hexagonal chicken-wire network shown in Fig. 1, without additional interpenetrating networks, it would possess cylindrical channels about 12–13 Å across.[16,18] In practice the empty chicken-wire network is not formed. A novel approach to prevent the formation of interpenetrating lattices was recently reported by Yaghi *et al.*[10] which involved the formation of hydrated metal-ion salts of H_3btc of composition $[M_3(btc)_2(H_2O)_{12}]$ (M = Co, Ni or Zn) in which the divalent metal ion bridges between the carboxylate groups. Dehydration of the metal ions gives a material with some porosity and leaves the metal ions lining the channels. Ionic bonds and most co-ordinative bonds are stronger than hydrogen bonds so in general may be more effective in stabilising a microporous lattice after creating a void volume either by removal of water or any other guests included during crystallisation. Furthermore for H_3btc crystallisation with divalent metal ions avoids the formation of an interpenetrating lattice and gives an open framework. Our long-term goal is the preparation of thermally and chemically stable open-framework solids and in particular microporous organic zeolites with a stable lattice based on ionic, co-ordinative and hydrogen bonding.

Results and Discussion

This paper reports the hydrothermal synthesis and single-crystal structure characterisation of $[M(Hbtc)(H_2O)_2]\cdot 0.5H_2O$ (M = Sr or Ba) which were prepared by heating H_3btc with $M^{II}(O_2CMe)_2$ in water in a sealed bomb. These are isostructural and similar in structure to the analogous calcium salt of formula $[Ca(Hbtc)(H_2O)]\cdot H_2O$ which we have already reported.[11] Alkaline-earth-metal salts of H_3btc were expected to be stable insoluble solids because of the insolubility of the corresponding carbonates. Calcium carbonate occurs as chalk, limestone and marble and is highly insoluble.[19] It is also cheap with many bulk commercial applications. Hydrothermal methods were used because the high temperature presumably allows total dissolution of the reagents, aiding the growth of good-quality crystalline material upon slow cooling. The salts were obtained in high yields and are indeed insoluble in water and dilute mineral acids. All three structures are in the form of alternating layers parallel to (0,0,1) of either anions or cations and water molecules stacked in the direction of *c* (Fig. 2). Hydrogen bonds link anions related by the cell translation $1 + x$, $1 + y$, z into chains perpendicular to (1,1,0) and crystallographic centres of symmetry relate adjacent chains within the anion layer. Thus within the layer the benzene rings of the Hbtc anions are all parallel to one another and carboxylic groups protrude from either side of the layer. The position of the hydrogen atom, which forms a hydrogen bond linking the Hbtc anions together, was determined in each case. For the barium and strontium salts its presence was confirmed from the stoichiometry of the compounds and by an IR stretch at 1696 cm^{-1} characteristic of an aromatic carboxylic acid group.

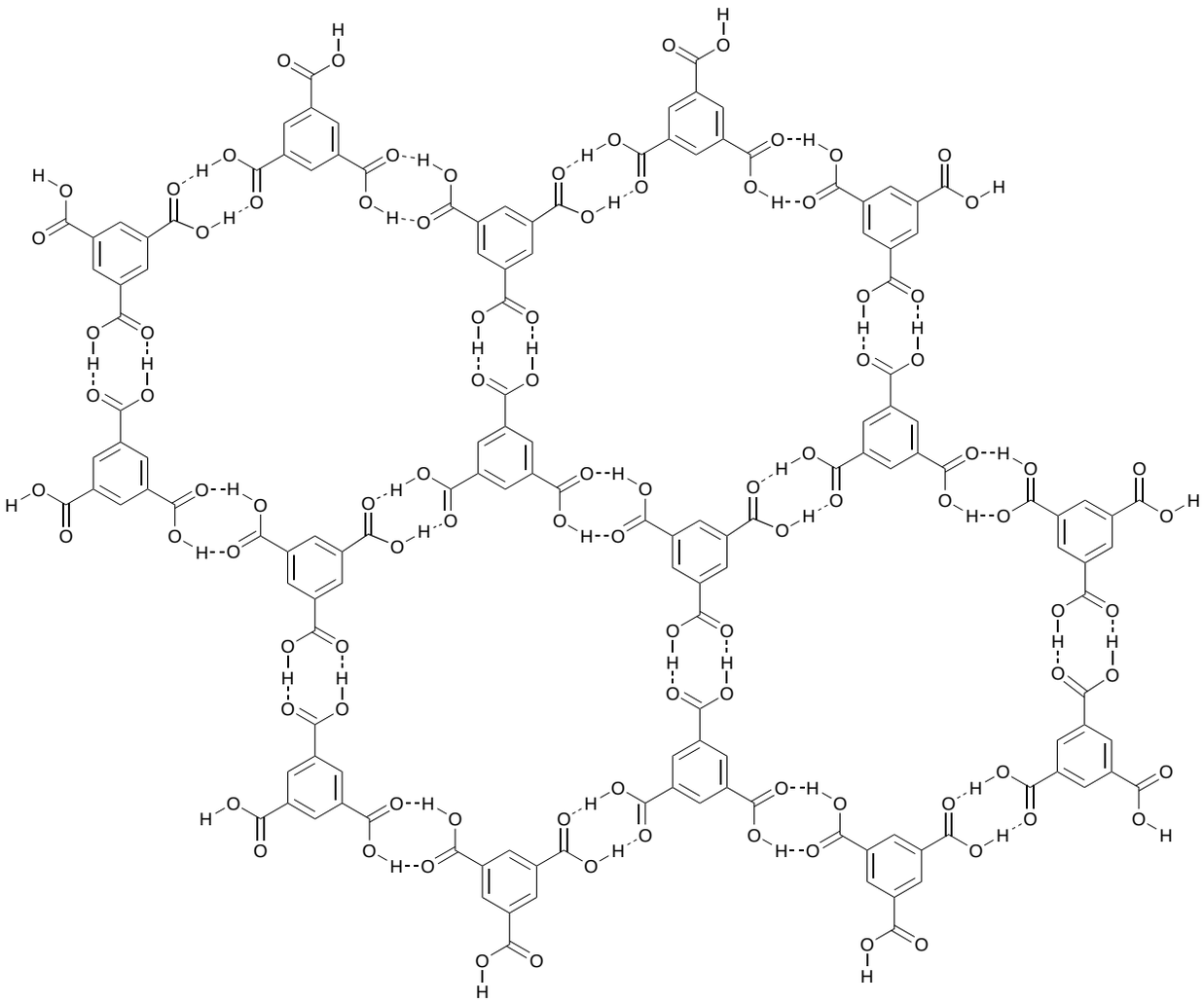

Fig. 1 Drawing of the hexagonal network formed from six H_3btc molecules connected by carboxylic acid hydrogen-bonded dimers

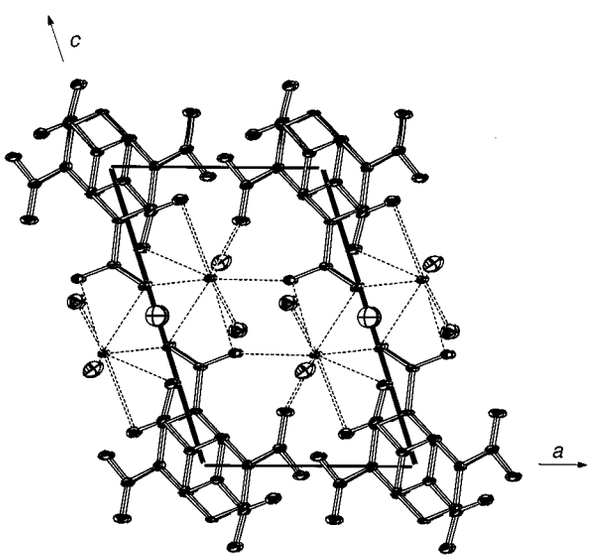

Fig. 2 Parallel perspective view of a portion of the structure of [Ba(Hbtc)$(H_2O)_2$]·0.5H_2O. The direction of view is along *b* which runs down into the page. Hydrogen atoms have been omitted for clarity and non-hydrogen atoms are represented by 40% probability ellipsoids and have coordinates in the range −0.5 to 1.5 for *x* and *y* and −0.3 to 1.3 for *z*. The atoms are not labelled but the use of dashed lines for Ba–O bonds and pairs of solid lines for bonds within the anions serve to identify the species present. The zeolitic water molecule (O3W) is readily identifiable because of its size and position at the mid point of the unit cell edge *c*

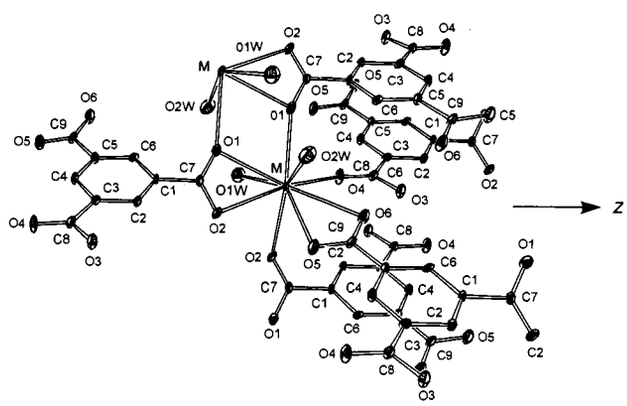

Fig. 3 Co-ordination of M in [M(Hbtc)$(H_2O)_2$]·0.5H_2O (M = Sr or Ba). Atoms are shown as 40% probability ellipsoids and selected atoms are labelled. Hydrogen atoms have been omitted for clarity

Furthermore the C8–O3 bonds [1.332(5) and 1.325(14) Å for Ba and Sr respectively] of the C8–O3–H3 carboxyl groups are comparatively long. There is significant departure from planarity of the Hbtc anions owing to rotation of the carboxylate groups out of the plane of the benzene ring. The rotation angles for the carboxylate groups in the order C7, C8 and C9, estimated from dihedral angles, are 37.2(6), 6.6(6) and 9.0(7)° for Ba and 41.3(12), 6.0(12) and 10.4(12)° for Sr. The Ba^{2+} and Sr^{2+} cations are co-ordinated to five distinct carboxylate anions, two acting as bidentate and three as monodentate ligands (Fig. 3). There are two water molecules in the co-ordination sphere

Table 1 Thermal gravimetric analyses; *ca.* 10 mg sample heated under a flow of nitrogen at 1 °C min^{-1} from 20 °C

	$[Ca(Hbtc)(H_2O)]\cdot H_2O$	$[Sr(Hbtc)(H_2O)_2]\cdot 0.5H_2O$	$[Ba(Hbtc)(H_2O)_2]\cdot 0.5H_2O$	$[Co(pdc)(H_2O)_2]$
% Weight loss	13.16	13.46	11.47	13.74
H_2O per molecule	2.06	2.53	2.47	1.99
Temperature range (°C)	45–170	29–165	35–175	115–175
Thermal stability	250	215	265–285	300–330

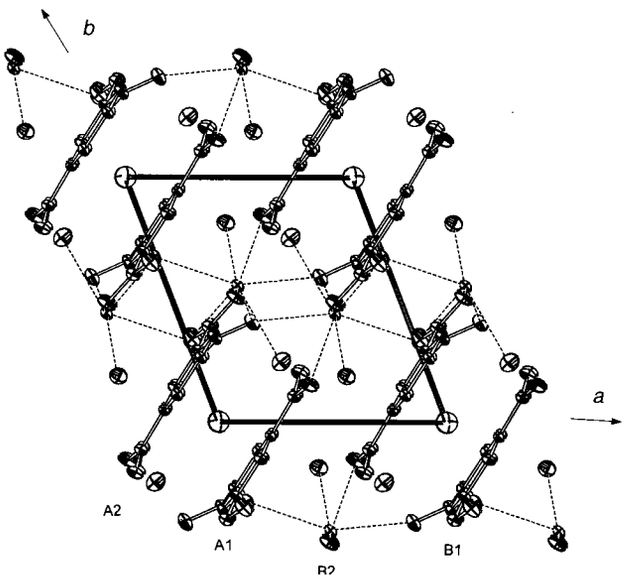

Fig. 4 Parallel perspective view down *c* which is orientated up out of the page. The annotations A1, A2, B1 and B2 identify specific sheets of cations and anions

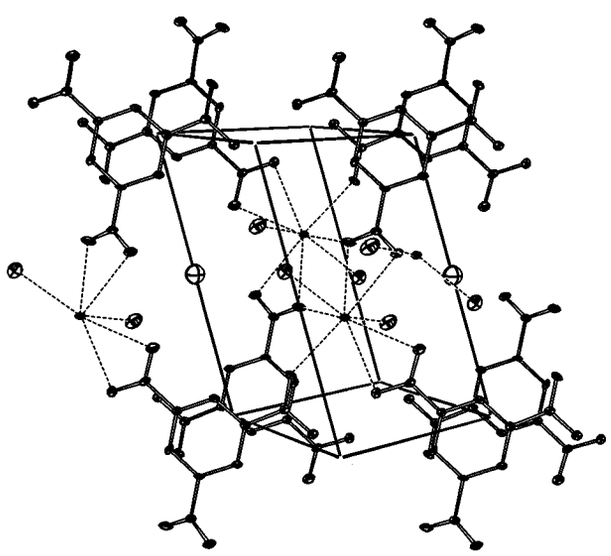

Fig. 5 Parallel perspective view of the layers (A1 and A2 in Fig. 4) of closely connected cations and anions projected on (−1,1,0). Hydrogens are omitted for clarity and non-hydrogen atoms are shown as 40% probability ellipsoids

with metal–oxygen bond lengths of 2.860(6) and 2.877(6) Å for Ba and 2.706(9) and 2.722(10) Å for Sr which reflect the different ionic radii of the metal cations. A third loosely bound zeolitic water molecule is also present at a crystallographic centre of symmetry.

The alternative view of the structure down *c* shown in Fig. 4 demonstrates that most of the atoms lie on or close to the (−220) planes except for the water molecules which lie between the layers. The spacing between the sheets corresponds to the *d* spacing of the planes (3.170 or 3.121 Å for Ba and Sr respectively) and hence the lattice is also stabilised by π stacking between the Hbtc tectons. Fig. 5 depicts two representative sheets (A1 and A2) from Fig. 4. Of particular interest is the large void surrounding the O3W water molecules which probably provides a pathway for the facile loss of water from the lattice on heating which is discussed below.

Table 1 shows the thermal gravimetric analysis results. Data for the previously reported salts $[Ca(Hbtc)(H_2O)]\cdot H_2O$ [11] and $[Co(pdc)(H_2O)_2]$ [13] (pdc = pyridine-3,5-dicarboxylate) are included for comparison. The solids show exceptionally good thermal stability compared to other co-ordination polymers based on co-ordinative bonding. The percentage weight loss corresponds to the total dehydration of the samples. The homogeneity of the original hydrated samples was shown by microanalysis and by the X-ray powder diffraction (XRPD) patterns which were in good agreement with those calculated from the single-crystal structure data. Fig. 6 shows the XRPD patterns for the strontium sample which gave the sharpest lines for the dehydrated and rehydrated samples.† The calculated powder pattern (*a*) is, with one exception, in excellent agreement with the pattern (*b*) obtained experimentally. The exception is the intensity of the line at 2θ 28.6° which is far too intense in the experimental pattern. This line corresponds to the −220 reflection which in turn relates directly to the sheets of cations and anions. The effect is therefore a consequence of preferred orientation of the crystallites in the preparation of the experimental powder diffraction pattern. The phenomenon is almost inevitable in the case of materials with a well defined layer structure such as clay minerals and it is not surprising that it is encountered here. Heating $[Sr(Hbtc)(H_2O)_2]\cdot 0.5H_2O$ at 175 °C for 4 h drives off the water to give an anhydrous salt whose powder diffraction pattern is shown in Fig. 6(*c*). This is clearly crystalline as shown by the sharp peaks but the powder pattern is completely different from that of the original hydrated compound. The new pattern can be completely and unambiguously indexed on the basis of a primitive monoclinic unit cell with $a = 13.025(8)$, $b = 4.8065(16)$ and $c = 15.986(7)$ Å, $\beta = 105.07(3)°$ and $U = 966.4$ Å^3. This is completely compatible with a cell content (Z) of four formula units of the anhydrous salt.‡ There is no obvious simple relationship between this monoclinic cell and the triclinic cell of the parent hydrate. This implies that a profound change of structure occurs on dehydration, although the lack of knowledge of the precise structure of the anhydrous salt precludes a detailed discussion of its nature. Suspending a sample of the anhydrous salt in cold water for 24 h completely rehydrates the salt to give the original structure as shown by the powder diffraction of the rehydrated salt [Fig. 6(*d*)] and by microanalysis. The pattern is in excellent agreement with that of the original hydrated compound subject only to the effect of preferred orientation observed previously. Upon dehydration and rehydration the water molecules are thought to move in a direction perpendicular to the sheets owing to the large void volume surrounding O3W. The crystal-

† Samples were dehydrated by heating in a tube furnace at 175 °C for 4 h. The sample weight was checked to ensure complete dehydration. Samples were rehydrated by submerging them in water for 24 h followed by drying in a desiccator over $CaCl_2$.

‡ The monoclinic cell of the anhydrous salt has been arrived at by indexing the lines of the powder diffraction pattern. This is an error-prone procedure and would be reinforced by more direct confirmatory evidence.

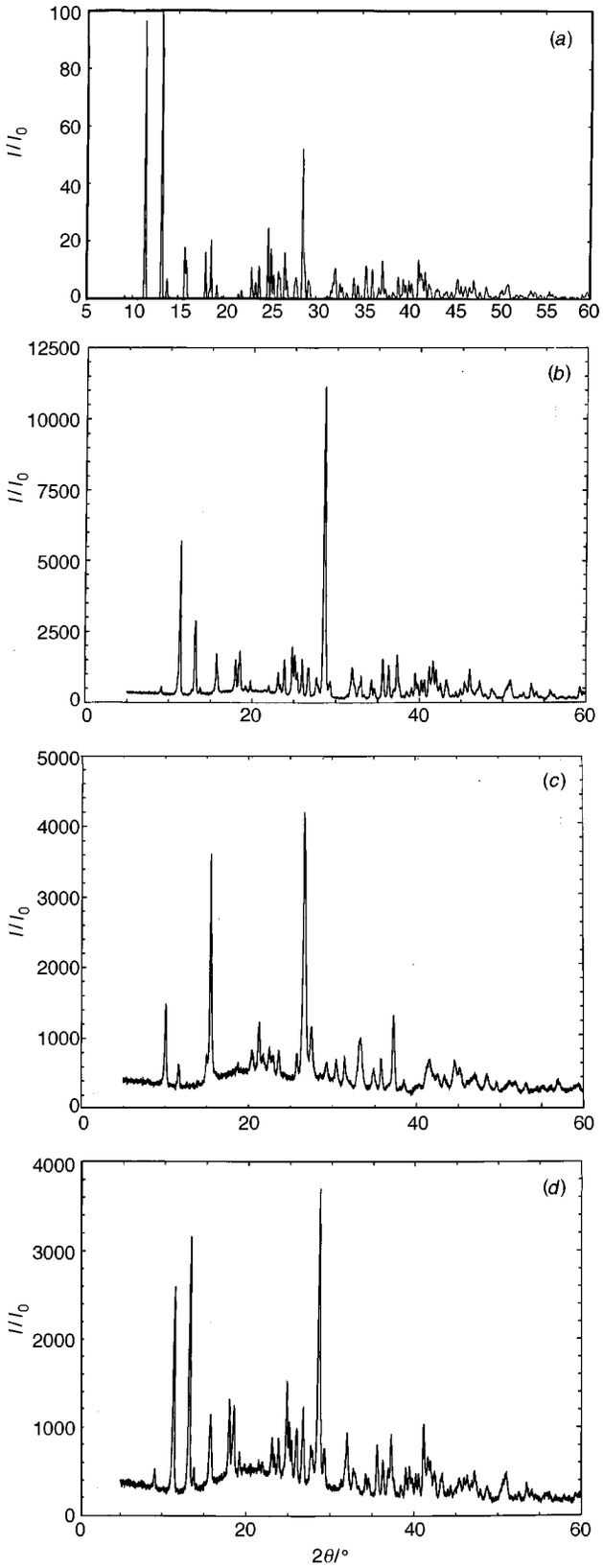

Fig. 6 Powder diffraction patterns for (*a*) $[Sr(Hbtc)(H_2O)_2]\cdot 0.5H_2O$ (calculated pattern), (*b*) $[Sr(Hbtc)(H_2O)_2]\cdot 0.5H_2O$, (*c*) [Sr(Hbtc)] (dehydrated sample) and (*d*) $[Sr(Hbtc)(H_2O)_2]\cdot 0.5H_2O$ (rehydrated sample)

linity of the dehydrated phase contrasts with the XRPD patterns reported for dehydrated samples of $[M_3(btc)_2(H_2O)_{12}]$ (M = Co, Ni or Zn) which showed considerable line broadening and loss of internal crystallinity.[10] The latter probably loses internal crystallinity more easily on dehydration because more water molecules per cation are liberated, creating more space, and the metal ions are not so extensively co-ordinated by carboxylate ligands.

Table 2 Results of BET/SEM studies*

Compound	Surface area/$m^2\ g^{-1}$
[Ca(Hbtc)]	1.58
[Sr(Hbtc)]	3.58
[Ba(Hbtc)]	1.86
$[Co_3(btc)_2(H_2O)]$	6.47
[Co(pdc)]	9.61

* Measurements were made using a Quantasorb instrument (Quantachrome Corporation, Syosset, NY) following the manufacturers standard recommended procedure (http://www.quantachrome.com/applicat.htm and http://www.quantachrome.com/). The instrument accuracy was checked with a standard sample of α-alumina (Certificate of Measurement, Certified Reference Material No. M11-05, Laboratory of the Government Chemist, Teddington, Middlesex).

Brunauer, Emmett and Teller[20] (BET) single-point surface-area measurements using a nitrogen-helium (30 : 70) gas mixture were performed on dehydrated samples and compared with results for some related samples to see if evidence for microporosity could be found by the absorption of nitrogen into the pores. The samples were degassed at 160 °C for 20 h under a nitrogen gas flow and then cooled to liquid-nitrogen temperature. Warming to room temperature liberates absorbed nitrogen gas which is determined by measuring the increase in nitrogen composition of the N_2–He carrier gas with a calibrated thermal conductivity detector. Scanning electron microscopy (SEM) was used to obtain a semi-quantitative measurement of the crystal size after the BET measurements had been performed. Fig. 7 shows the electron micrograph photographs. The results are summarised in Table 2. For [M(Hbtc)] (M = Ca, Sr or Ba) no internal surface area is observed as the surface-area measurement can be accounted for by the external surface area. Nitrogen and water molecules are of similar size so presumably upon dehydration the lattice may rearrange to minimise the void volume which explains why nitrogen cannot penetrate the lattice. On rehydration the water molecules will co-ordinate to the metal ions, expanding the lattice to its original shape. However, the $[Co_3(btc)_2(H_2O)]$[10] and [Co(pdc)][13b] samples showed much larger surface areas suggesting that nitrogen can penetrate the pores. The dehydrated sample of [Co(pdc)] has a BET surface area of 10 $m^2\ g^{-1}$ which is five times greater than that of [Ca(Hbtc)]. These values are however much lower than what might have been expected for the internal surface area alone. For example if each salt had absorbed 1 mol of nitrogen to give $[M(Hbtc)]\cdot N_2$ (M = Ca, Sr or Ba), $[Co(pdc)]\cdot N_2$ and $[Co_{1.5}(btc)(H_2O)_{0.5}]\cdot N_2$, and liberated this on warming, the corresponding BET surface areas would be 393, 330, 283, 436 and 321 $m^2\ g^{-1}$ respectively. (The BET cross-sectional area of nitrogen forming a monolayer was taken as 16.2×10^{-20} m^2 per molecule. Estimated values = cross-sectional area of nitrogen × Avogadro's constant/molecular weight of salt.) To the best of our knowledge this is the first report of surface-area measurements for crystalline organic molecular co-ordination polymers.

Conclusion

Heating alkaline-earth-metal acetates with H_3btc gives non-interpenetrating ionic lattice networks which can be dehydrated and rehydrated reversibly. Dehydration changes the lattice structure, probably reducing the pore volume which prevents the absorption of nitrogen. Rehydration appears to reverse these changes. These studies exemplify the difficulty of forming genuine organic zeolites which maintain their structural integrity and have micropores after the removal of water molecules from the metal-ion co-ordination sphere. Evidence for micro-

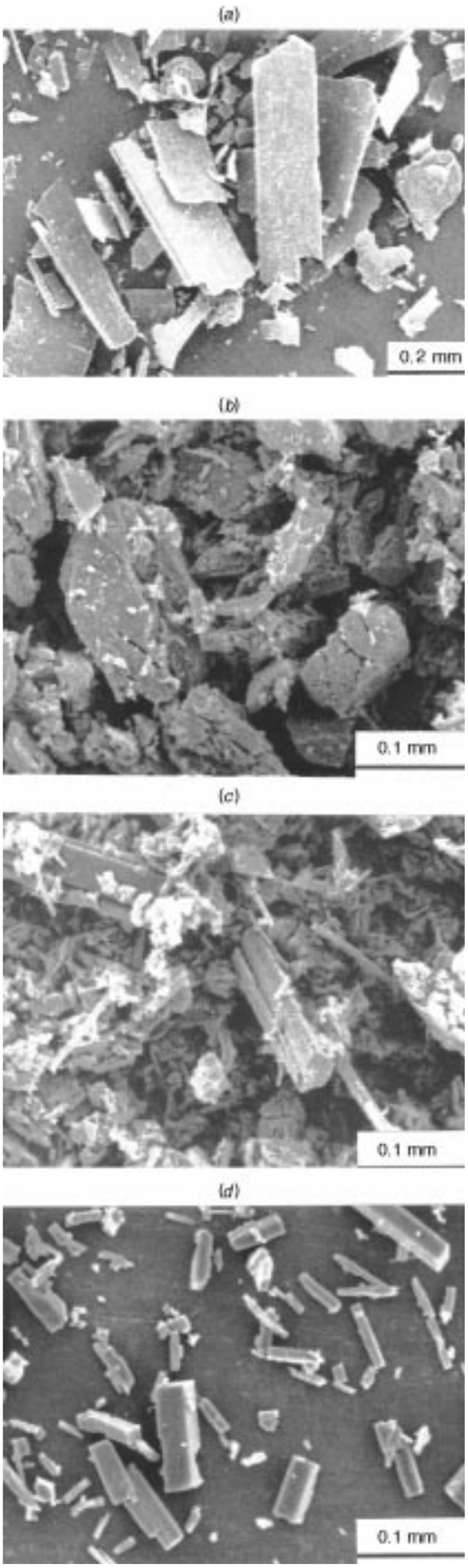

Fig. 7 Electron micrograph photographs after BET measurements of (*a*) [Ca(Hbtc)], (*b*) [Sr(Hbtc)], (*c*) [Ba(Hbtc)] and (*d*) [Co(pdc)]

pores in co-ordination polymers is probably best obtained by studying the absorption of neutral non-co-ordinating atoms or molecules. Future studies will use larger aromatic tectons as building blocks to study the effect of metal–ligand co-ordination, hydrogen bonding, π stacking and guest inclusion on lattice stabilisation.

Experimental

Preparations

The compounds H_3btc (Aldrich) (350 mg, 1.67 mmol) and $Sr(O_2CMe)_2$ (Aldrich) (343 mg, 1.67 mmol) in water (25 cm^3) were sealed in a Teflon-lined safety bomb (45 cm^3) (Scientific and Medical Products Ltd., Manchester) and placed in an oven at 180 °C. After about 10 h the oven temperature was slowly turned down over a 36 h period to 80 °C and then allowed to cool to room temperature. Colourless crystals were collected, washed with distilled water and dried over $CaCl_2$ in a desiccator (445 mg, 78%). The barium salt was made in an analogous manner (535 mg, 82%) {Found: C, 31.9; H, 2.2; Sr, 25.7. $[Sr(Hbtc)(H_2O)_2]\cdot 0.5H_2O$ requires C, 31.7; H, 2.6; Sr, 25.7. Found: C, 27.8; H, 1.9; Ba, 35.7. $[Ba(Hbtc)(H_2O)_2]\cdot 0.5H_2O$ requires C, 27.7; H, 2.3; Ba, 35.2%}.

Crystallography

A colourless crystal of $[Sr(Hbtc)(H_2O)_2]\cdot 0.5H_2O$ (0.3 × 0.18 × 0.14 mm) was mounted with superglue on a glass fibre. Crystal data: triclinic, space group $P\bar{1}$ (no. 2), with $a = 7.266(10)$, $b = 8.368(14)$, $c = 10.163(11)$ Å, $\alpha = 94.81(11)$, $\beta = 105.18(9)$, $\gamma = 109.18(13)°$, $U = 553.4(14)$ Å^3, $Z = 2$, $D_c = 2.045$ Mg m^{-3}, $2\theta_{max} = 60.0°$, Mo-Kα radiation ($\lambda = 0.710\ 73$ Å), θ–2θ scan mode, μ(Mo-Kα) = 4.910 mm^{-1}. A total of 3247 independent reflections were collected at 298 K. A colourless crystal of $[Ba(Hbtc)(H_2O)_2]\cdot 0.5H_2O$ (0.4 × 0.3 × 0.2 mm) was mounted with superglue on a glass fibre. Crystal data: triclinic, space group $P\bar{1}$ (no. 2), $a = 7.481(8)$, $b = 8.336(10)$, $c = 10.420(9)$ Å, $\alpha = 93.56(8)$, $\beta = 105.39(8)$, $\gamma = 109.35(9)°$, $U = 583.0(11)$ Å^3, $Z = 2$, $D_c = 2.224$ Mg m^{-3}, $2\theta_{max} = 60.0°$, Mo-Kα radiation ($\lambda = 0.710\ 73$ Å), θ–2θ scan mode, μ(Mo-Kα) = 3.443 mm^{-1}. A total of 3428 reflections were collected at 298 K which reduced to 3427 independent reflections.

Except where noted the same conditions apply to both structure determinations. Data were collected using Nicolet P3 software and 2θ scan rates of 5.33 ($I_p < 150$) to 58.6° min^{-1} ($I_p > 2500$) where I_p is the prescan intensity. Scan widths were 2θ 2.4 to 2.7°. During data collection no decay was observed. Data reduction used an RDNIC data reduction program for the Nicolet P3 diffractometer.[21] An empirical absorption correction based on ψ scans was applied in both cases.[22]

The structure of the barium salt was solved by direct methods in the non-centrosymmetric space group $P1$ (no. 1) to yield positions for all non-hydrogen atoms except for O3W. It was immediately apparent that the structure was in fact centrosymmetric. After appropriate adjustment of the coordinates, refinement was carried out by full-matrix least squares in the centrosymmetric space group $P\bar{1}$ during which O3W was found in a difference map. The non-hydrogen atom positional parameters found for the barium salt were used directly as starting coordinates for the strontium salt. For both structures all the non-hydrogen atoms except O3W were refined anisotropically. The presence of the high atomic number cations and disorder precluded determination of the positions of the hydrogens of the water molecules. The aryl and hydroxyl hydrogens were placed in calculated positions and refined with a riding model. Both structures exhibited large peaks and holes in the final difference maps (2.676 and −2.560 and 6.802 and −4.667 e Å^{-3} for Sr and Ba respectively) at 1.0 Å from the cations. These are attributed to ripple caused by series terminations. While the R values for the barium salt ($R = 0.057$, $wR2 = 0.159$, $S = 1.072$)

are acceptable those for Sr are rather high ($R1 = 0.097$, $wR2 = 0.296$, $S = 1.056$). This is attributed to limitations in the intensity data available for Sr due in part to the comparatively small crystal used compounded by the presence of a significant amount of Sr and the use of Mo-Kα radiation. This is a well known source of difficulty.

All computations were performed on the SUN SPARCserver (UNIX operating system) of the computing centre of the University of Aberdeen. Structure solution and refinement used the programs SHELXS 86[23] and SHELXL 93.[24] Molecular graphics were prepared using the ORTEX program.[25]

CCDC reference number 186/847.

Acknowledgements

We are grateful to Professor F. P. Glasser for helpful discussions.

References

1 (*a*) M. J. Zaworotko, *Chem. Soc. Rev.*, 1994, **23**, 283; (*b*) R. Robson and B. F. Hoskins, *J. Am. Chem. Soc.*, 1990, **112**, 1546; (*c*) R. Robson, B. F. Abrahams, S. R. Batten, R. W. Gable, B. F. Hoskins and J. Liu, *Supramolecular Architecture*, American Chemical Society, Washington, DC, 1992, ch. 19; (*d*) G. R. Desiraju, *Crystal Engineering*, *The Design of Organic Solids*, Elsevier, Amsterdam, 1989; (*e*) D. Venkataraman, G. B. Gardner, S. Lee and J. S. Moore, *Nature* (*London*), 1995, **374**, 792.

2 (*a*) S. W. Keller, *Angew. Chem.*, 1997, **109**, 295; *Angew. Chem.*, *Int. Ed. Engl.*, 1997, **36**, 247; (*b*) A. Dyer, *An Introduction to Zeolite Molecular Sieves*, Wiley, Chichester, 1988.

3 (*a*) L. Carlucci, G. Ciani, D. M. Proserpio and A. Sironi, *Inorg. Chem.*, 1995, **34**, 5698; (*b*) J. Lu, T. Paliwala, S. C. Lim, C. Yu, T. Niu and A. J. Jacobson, *Inorg. Chem.*, 1997, **36**, 923.

4 P. Losier and M. J. Zaworotko, *Angew. Chem.*, *Int. Ed. Engl.*, 1996, **35**, 2779; S. Kitagawa, M. Kondo, T. Yoshitomi, K. Seki and H. Matsuzaka, *Angew. Chem.*, *Int. Ed. Engl.*, 1997, **36**, 1725.

5 (*a*) O. M. Yaghi and H. Li, *J. Am. Chem. Soc.*, 1995, **117**, 10 401; (*b*) O. M. Yaghi and G. Li, *Angew. Chem.*, *Int. Ed. Engl.*, 1995, **34**, 207.

6 M. J. Zaworotko and S. Subramanian, *Angew. Chem.*, *Int. Ed. Engl.*, 1995, **34**, 2127; P. S. Halasyamani, M. J. Drewitt and D. O'Hare, *Chem. Commun.*, 1997, 867.

7 M. Fujita, Y. Kwon, S. Washizu and K. Ogura, *J. Am. Chem. Soc.*, 1994, **116**, 1151.

8 R. Robson, S. R. Batten and B. F. Hoskins, *J. Am. Chem. Soc.*, 1995, **117**, 5385.

9 B. F. Abrahams, M. J. Hardie, B. F. Hoskins, R. Robson and E. E. Sutherland, *J. Chem. Soc.*, *Chem. Commun.*, 1994, 1049.

10 O. M. Yaghi, H. Li and T. L. Groy, *J. Am. Chem. Soc.*, 1996, **118**, 9096.

11 M. J. Plater, A. J. Roberts and R. A. Howie, *Chem. Commun.*, 1997, 893.

12 (*a*) S. O. H. Gutschke, M. Molinier, A. K. Powell and P. T. Wood, *Angew. Chem.*, *Int. Ed. Engl.*, 1997, **36**, 991; (*b*) C. Robl and A. Weiss, *Z. Naturforsch.*, *Teil B*, 1986, **41**, 1485; (*c*) D. Deguenon, G. Bernardinelli, J. Tuchagues and P. Castan, *Inorg. Chem.*, 1990, **29**, 3031; (*d*) C. Robl and A. Weiss, *Z. Naturforsch.*, *Teil B*, 1986, **41**, 1495.

13 (*a*) S. O. H. Gutschke, A. M. Z. Slawin and P. T. Wood, *J. Chem. Soc.*, *Chem. Commun.*, 1995, 2197; (*b*) M. J. Plater, R. A. Howie and A. J. Roberts, *J. Chem. Res.*, in press.

14 O. M. Yaghi, G. Li and H. Li, *Nature* (*London*), 1995, **378**, 703.

15 D. Venkataraman, G. B. Gardner, S. Lee and J. S. Moore, *J. Am. Chem. Soc.*, 1995, **117**, 11 600.

16 D. J. Duchamp and R. E. Marsh, *Acta Crystallogr.*, *Sect. B*, 1969, **25**, 5.

17 O. Ermer, *J. Am. Chem. Soc.*, 1988, **110**, 3747.

18 J. E. D. Davies, P. Finocchiaro and F. H. Herbstein, *Inclusion Compounds*, eds. J. L. Atwood, J. E. D. Davies and D. D. MacNicol, Academic Press, New York, 1984, vol. 2, pp. 407–419.

19 N. N. Greenwood and A. Earnshaw, *Chemistry of the Elements*, Pergamon, Oxford, 1984, p. 119.

20 S. Brunauer, P. H. Emmett and E. Teller, *J. Am. Chem. Soc.*, 1939, **60**, 309.

21 R. A. Howie, University of Aberdeen, 1980.

22 A. C. T. North, D. C. Phillips and F. S. Matthews, *Acta Crystallogr.*, *Sect. A*, 1968, **24**, 351.

23 G. M. Sheldrick, *Acta Crystallogr.*, *Sect. A*, 1990, **46**, 467.

24 G. M. Sheldrick, SHELXL 93, Program for the Refinement of Crystal Structures, University of Göttingen, 1993.

25 P. McArdle, *J. Appl. Crystallogr.*, 1994, **27**, 438.

Received 13*th November* 1997; *Paper* 7/08189H